



UNIVERSITY OF LEEDS

This is a repository copy of *Tectonic controls on the long-term carbon isotope mass balance*.

White Rose Research Online URL for this paper:
<http://eprints.whiterose.ac.uk/114569/>

Version: Accepted Version

Article:

Shields, GA and Mills, BJW orcid.org/0000-0002-9141-0931 (2017) Tectonic controls on the long-term carbon isotope mass balance. *Proceedings of the National Academy of Sciences*, 114 (17). pp. 4318-4323. ISSN 1091-6490

<https://doi.org/10.1073/pnas.1614506114>

© National Academy of Sciences 2017. This is an author produced version of a paper published in *Proceedings of the National Academy of Sciences*. Uploaded in accordance with the publisher's self-archiving policy. In order to comply with the publisher requirements the University does not require the author to sign a non-exclusive licence for this paper.

Reuse

Items deposited in White Rose Research Online are protected by copyright, with all rights reserved unless indicated otherwise. They may be downloaded and/or printed for private study, or other acts as permitted by national copyright laws. The publisher or other rights holders may allow further reproduction and re-use of the full text version. This is indicated by the licence information on the White Rose Research Online record for the item.

Takedown

If you consider content in White Rose Research Online to be in breach of UK law, please notify us by emailing eprints@whiterose.ac.uk including the URL of the record and the reason for the withdrawal request.



eprints@whiterose.ac.uk
<https://eprints.whiterose.ac.uk/>

Tectonic controls on the long-term carbon isotope mass balance

Graham A. Shields¹ and Benjamin J. W. Mills²

¹Department of Earth Sciences, University College London, Gower Street, London WC1E 6BT, UK; g.shields@ucl.ac.uk ²School of Earth and Environment, University of Leeds, Leeds LS2 9JT, UK; b.mills@leeds.ac.uk

Submitted to Proceedings of the National Academy of Sciences of the United States of America

The long-term, steady-state marine carbon isotope record reflects changes to the proportional burial rate of organic carbon relative to total carbon on a global scale. For this reason, times of high $\delta^{13}\text{C}$ are conventionally interpreted to be oxygenation events caused by excess organic burial. Here we show that the carbon isotope mass balance is also significantly affected by tectonic uplift and erosion via changes to the inorganic carbon cycle that are independent of changes to the isotopic composition of carbon input. This view is supported by inverse co-variance between $\delta^{13}\text{C}$ and a range of uplift proxies, including seawater $^{87}\text{Sr}/^{86}\text{Sr}$, that demonstrates how erosional forcing of carbonate weathering outweighs that of organic burial on geological time scales. A model of the long-term carbon cycle shows that increases in $\delta^{13}\text{C}$ need not be associated with increased organic burial and that alternative tectonic drivers (erosion, outgassing) provide testable and plausible explanations for sustained deviations from the long-term $\delta^{13}\text{C}$ mean. Our approach emphasizes the commonly overlooked difference between how net and gross carbon fluxes affect the long-term carbon isotope mass balance, and may lead to reassessment of the role that the $\delta^{13}\text{C}$ record plays in reconstructing the oxygenation of Earth's surface environment.

carbon isotopes | mass balance | tectonics | carbonate weathering | long-term carbon cycle

Introduction

Earth's highly oxygenated atmosphere derives largely from the splitting of the water molecule during photosynthesis. Respiration and decay reverse this process, consuming oxygen, but the burial of organic matter in sediments allows oxygen to accumulate in the atmosphere. Net oxygenation may also arise from burial of reduced sulphur species, but the organic carbon burial flux has been the major source of oxygen throughout the Phanerozoic (1-6).

Because photosynthesis results in ^{13}C -depleted organic carbon, the carbon isotope composition of past oceans has played an important role in tracing the oxygenation of Earth's surface environment. The conventional interpretation of C-isotope mass balance (7) presumes that prolonged intervals of high carbonate $\delta^{13}\text{C}$ are the result of elevated rates of organic carbon burial (removing a larger fraction of ^{13}C -depleted organic matter), and so correspond to an excess of oxygen production over consumption, which is in large part due to the oxidation of organic matter during surface weathering. This paradigm has led to the view that atmospheric oxygen levels rose at three crucial junctures in Earth history: at ~ 2.1 Ga (8-9), ~ 0.8 Ga (10-11) and ~ 0.3 Ga (7,12), and this has become generally accepted (13).

This paradigm encounters difficulties. Firstly, although Earth's oxygenation history does not rely solely on carbon isotope data, it is remarkable that independent evidence for oxygenation does not always coincide with high $\delta^{13}\text{C}$ (14). The Ediacaran-Cambrian faunal radiation (Cambrian Explosion), which is commonly attributed to oxygenation, is strangely accompanied by low, rather than high $\delta^{13}\text{C}$ (Fig. 1), while the many fluctuations in atmospheric oxygen between 15% and 32% that have been

identified using the Phanerozoic carbon isotope record (12), lack corroborating evidence (14). Although such inconsistencies are widely acknowledged, alternative explanations to explain global trends in $\delta^{13}\text{C}$ are uncommon. One possibly viable alternative attributes $\delta^{13}\text{C}$ fluctuations to the amount of diagenetically precipitated (and isotopically light) carbonate cement worldwide (14-15). Such large changes remain unsubstantiated, while the link to the global carbon cycle must appeal to a sampling bias, wherein a great mass of isotopically light material can be buried (to drive a positive excursion) yet does not lower the bulk isotopic composition of the carbonates which are analyzed. We argue that the preservation of a $\delta^{13}\text{C}$ signal that is correlated with other global processes is evidence against such sampling errors, and must be the result of definable system interactions (Fig. 1).

A second problem stems from the driving mechanism for increased organic burial during times of high $\delta^{13}\text{C}$. It is widely supposed that higher rates of organic burial are caused by increased nutrient input and/or sedimentation rates through weathering and erosion (5,11,16-17). However, long-term carbon isotope trends exhibit low, not high values during the collisional phases of supercontinent formation, while $\delta^{13}\text{C}$ shows an unexpected inverse relationship with erosion proxies, such as seawater $^{87}\text{Sr}/^{86}\text{Sr}$ and reconstructed sediment masses (Fig. 1, see SI for correlations), best illustrated by the Ediacaran-Ordovician orogenic interval of exceptionally high sedimentary fluxes, which are independently verified by zircon isotope studies (see SI). The C isotope record implies therefore that erosional forcing of organic burial does not control the long-term C isotope mass balance, and

Significance

The carbon isotope record has played a major role in reconstructing the oxygen and carbon dioxide content of the ancient atmosphere. However, known oxygenation events are not always reflected in the isotopic record of marine carbonate rocks, while conventional interpretations imply that less organic matter is buried when erosion rates are high, which is hard to explain. Here we show that both issues can be resolved if limestone weathering makes up a proportionately greater fraction of the global carbon cycle at high erosion rates. We argue that the link between carbon isotopes and oxygenation is more tenuous than commonly assumed, and propose a case-by-case re-examination of Earth's oxygenation history.

Reserved for Publication Footnotes

137
138
139
140
141
142
143
144
145
146
147
148
149
150
151
152
153
154
155
156
157
158
159
160
161
162
163
164
165
166
167
168
169
170
171
172
173
174
175
176
177
178
179
180
181
182
183
184
185
186
187
188
189
190
191
192
193
194
195
196
197
198
199
200
201
202
203
204

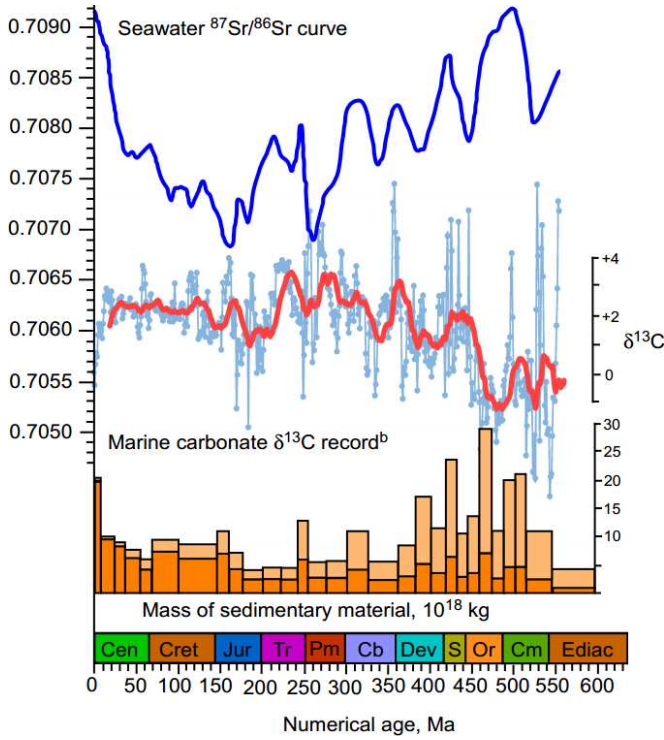


Fig. 1. Phanerozoic records of marine carbonate $\delta^{13}\text{C}$ (33), seawater Sr isotope composition (33) and mass of sedimentary material (two shades correspond to measured and estimated total mass, respectively) (34). Diverse tectonic proxies identify the Ediacaran-Ordovician interval as a time of maximal uplift and erosion, but minimal $\delta^{13}\text{C}$ (see SI).

that any such effect may be outweighed by an erosional forcing of carbonate burial.

The long-term carbon isotope mass balance

Figure 2 shows a representation of the long-term carbon cycle, which forms the basis for isotope mass balance calculations (18). Carbon enters the atmosphere/ocean system by four routes: oxidative weathering of fossil carbon (F_{wg}), carbonate weathering (F_{wc}) and metamorphic degassing of sedimentary organic carbon (F_{mg}) and carbonates (F_{mc}). Carbon leaves the surface pool via burial of organic carbon (F_{bg}) and inorganic carbonates (F_{bc}), with the fraction of total burial leaving via the organic route denoted f_{org} . The dashed lines in figure 2 show an important difference between net (solid lines) and gross (all lines) fluxes in the carbon cycle, which arises because the carbonate weathering-precipitation cycle is a CO_2 neutral process on long time-scales (19) (see SI).

The C-isotope mass balance (eq. 1) is based around the principle that on time scales greater than the residence time of carbon in the ocean (about 10^5 years), the quantity and isotopic composition of carbon entering and exiting the atmosphere-ocean system (A) must be the same (18):

$$\delta^{13}\text{C}_{in} = \delta^{13}\text{C}_{org} f_{org} + \delta^{13}\text{C}_{carb} (1 - f_{org}) \quad (1)$$

Standard calculations then assume that the average isotopic composition of carbon input ($\delta^{13}\text{C}_{in}$) is constant and approximately equal to $\delta^{13}\text{C}_{mantle}$ or about $-6\% \pm 1\%$. Rearranging equation (1) then allows the proportion of carbon buried as organic matter (f_{org}) to be read directly from the carbonate C isotope record (20). Knowledge of f_{org} , and the total input (\approx output) rate of carbon, F_{total} , then allows the rate of organic carbon burial, and hence oxygen production to be estimated (9,10):

$$F_{bg} = F_{total} \times (\delta^{13}\text{C}_{carb} - \delta^{13}\text{C}_{in}) / \Delta B \quad (2)$$

Following this reasoning, positive $\delta^{13}\text{C}$ excursions are commonly interpreted as organic C burial events, whereby the resul-

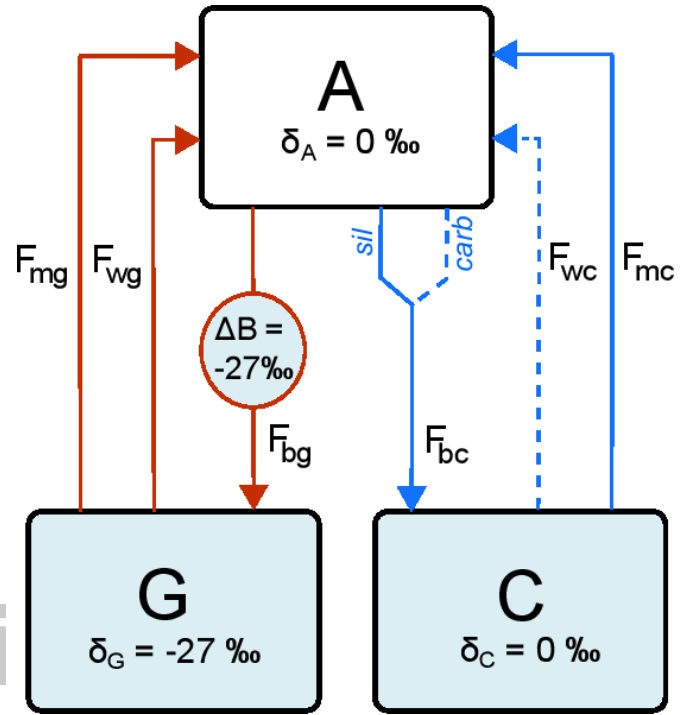


Fig. 2. Long term carbon cycle showing isotope fractionation. A is atmosphere and ocean carbon, G is buried organic carbon and C is buried carbonate carbon. F_b refers to burial fluxes, F_w to weathering and F_m to metamorphic/degassing fluxes. δ_x denotes the isotopic fractionation of reservoir X, and ΔB is the fractionation effect applied to buried organic carbon, taken to represent an average value over the Phanerozoic (35). *sil* and *carb* show alkalinity fluxes from silicate and carbonate weathering, respectively, which are combined to calculate F_{bc} (see SI). Dashed lines denote the 'null' carbonate weathering – deposition cycle.

tant oxygenation is quantified using the assumptions that total C throughput and net fluxes (the net carbon flux on geological time scales excludes the carbonate weathering flux) were similar to the present day, and that f_{org} approximates the proportion of outgassed CO_2 (including weathering sources) that is reduced to organic carbon (9,15). For example, the sustained baseline increase of $\sim 5\text{-}6\%$ during the early Neoproterozoic (11) is interpreted to imply an approximate doubling of organic burial due to increased phytoplankton body size (10) or high sedimentation rates (11). For the ~ 2.1 Ga Lomagundi Event of high $\delta^{13}\text{C}$, the total excess oxygen produced has been estimated at a massive 12-22 times the present inventory of atmospheric oxygen (8,9), with organic burial rates thought to increase by >20 times over the course of the isotope excursion (21).

Such large increases in organic carbon burial are difficult to reconcile with the operation of the long-term carbon cycle. Whilst organics contribute only around 20-25% of gross carbon burial (i.e. $f_{org} \approx 0.20\text{-}0.25$), they constitute more than 50% (19,6) and even as much as 72% (22) of the net carbon sink. Even a doubling of global organic carbon burial over geological timescales would therefore require a massive reorganization of the carbon cycle, alongside a contemporaneous increase in carbon sources through weathering and degassing, due to the impossibility of the other net sink (carbonate deposition following silicate weathering) being reduced below zero.

A physical erosion control on the carbon isotope mass balance

We propose here that long-term variation in f_{org} , and hence $\delta^{13}\text{C}$, may sometimes be driven by changes in the inorganic, rather than the organic side of the carbon cycle. Because the

205
206
207
208
209
210
211
212
213
214
215
216
217
218
219
220
221
222
223
224
225
226
227
228
229
230
231
232
233
234
235
236
237
238
239
240
241
242
243
244
245
246
247
248
249
250
251
252
253
254
255
256
257
258
259
260
261
262
263
264
265
266
267
268
269
270
271
272

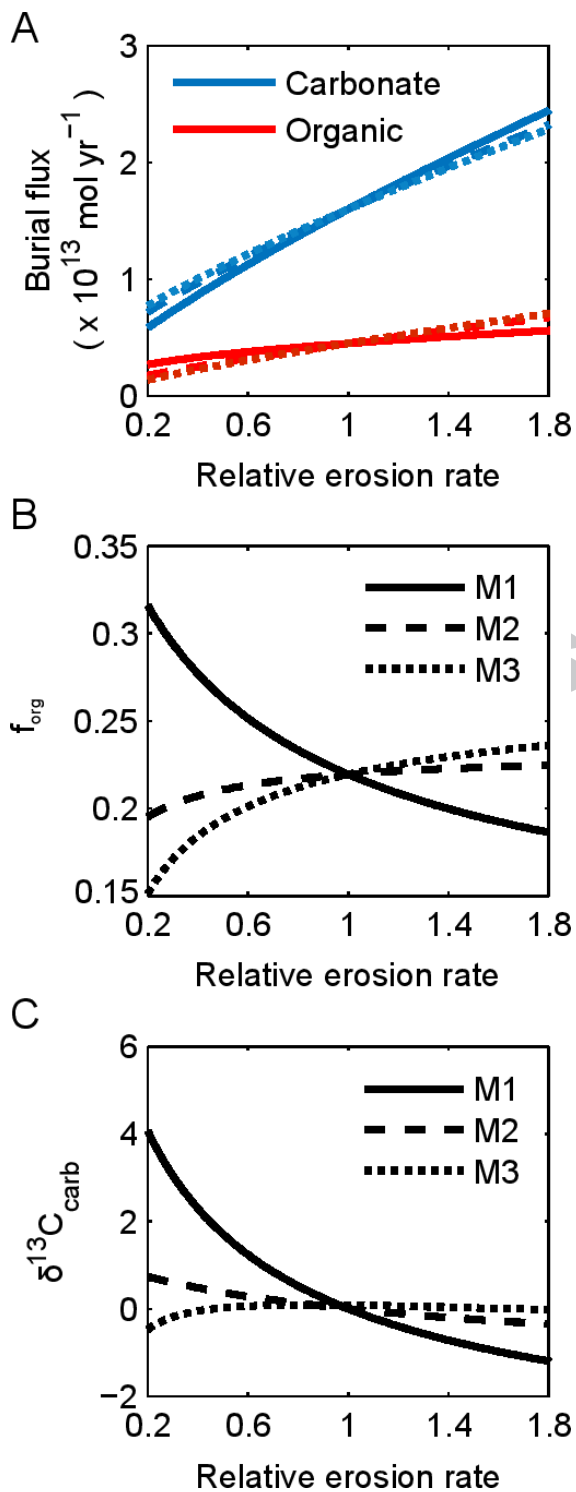


Fig. 3. Steady states of the long-term carbon cycle model. The system shown in Figure 2 is run to steady state for different values of the relative global uplift/erosion rate. Bold lines (M1) show results when silicate weathering delivers around 58% of ocean phosphate (29, see SI), dashed lines (M2) show results when silicate weathering delivers only 17% of ocean phosphate (6), and dotted lines (M3) show results when all P delivery is instead from carbonate weathering. The equations governing the response of fluxes to reservoir sizes and global temperature follow current models (6, 26). See SI for full model description, MATLAB code, and further evaluation.

carbonate weathering – deposition cycle is CO_2 neutral on time scales relevant to the C-isotope mass balance, increasing the

carbonate weathering (and deposition) rates acts to decrease f_{org} without impacting the net carbon fluxes responsible for driving climate. Although this is not the first study to link changes in carbonate weathering to $\delta^{13}\text{C}$, for example, it has been shown that a transient increase in carbonate weathering rates would drive an increase in $\delta^{13}\text{C}_{\text{in}}$ (23), our proposition differs from previous work by highlighting how sustained changes in carbonate deposition rates can alter f_{org} directly.

Such changes in the inorganic carbon cycle may be brought about by variation in erosion rates, driving step changes in carbonate weathering, and therefore gross carbon throughput. Whilst changes in erosion rate may also initially affect the net fluxes of silicate weathering and organic C burial, these must eventually return to balance the carbon cycle at steady state via temperature and nutrient feedbacks. There is no such requirement for carbonate weathering. This key difference between the net and gross carbon fluxes may explain why the erosional forcing of organic burial does not keep pace with carbonate burial during the early Palaeozoic and other orogenic events (Fig. 1).

Considering that mountains dominate global denudation rates (24), and that carbonate weathering is proportionately more important at higher erosion rates (25), we argue that f_{org} (and hence the $\delta^{13}\text{C}$ composition of the atmosphere-ocean system) will be lowered by tectonic uplift and erosion, unless compensated for by increased rates of net carbon flux (outgassing). Conversely, during periods of low denudation rates, $\delta^{13}\text{C}$ values will tend to be higher, although the overall weathering flux and organic burial rates may be lower. This is apparent when considering the evidence for low $\delta^{13}\text{C}$ during times of supercontinent formation and high $\delta^{13}\text{C}$ during times of supercontinent stability (16, 26), and can be observed by rearranging equation (2), assuming that erosion affects F_{total} :

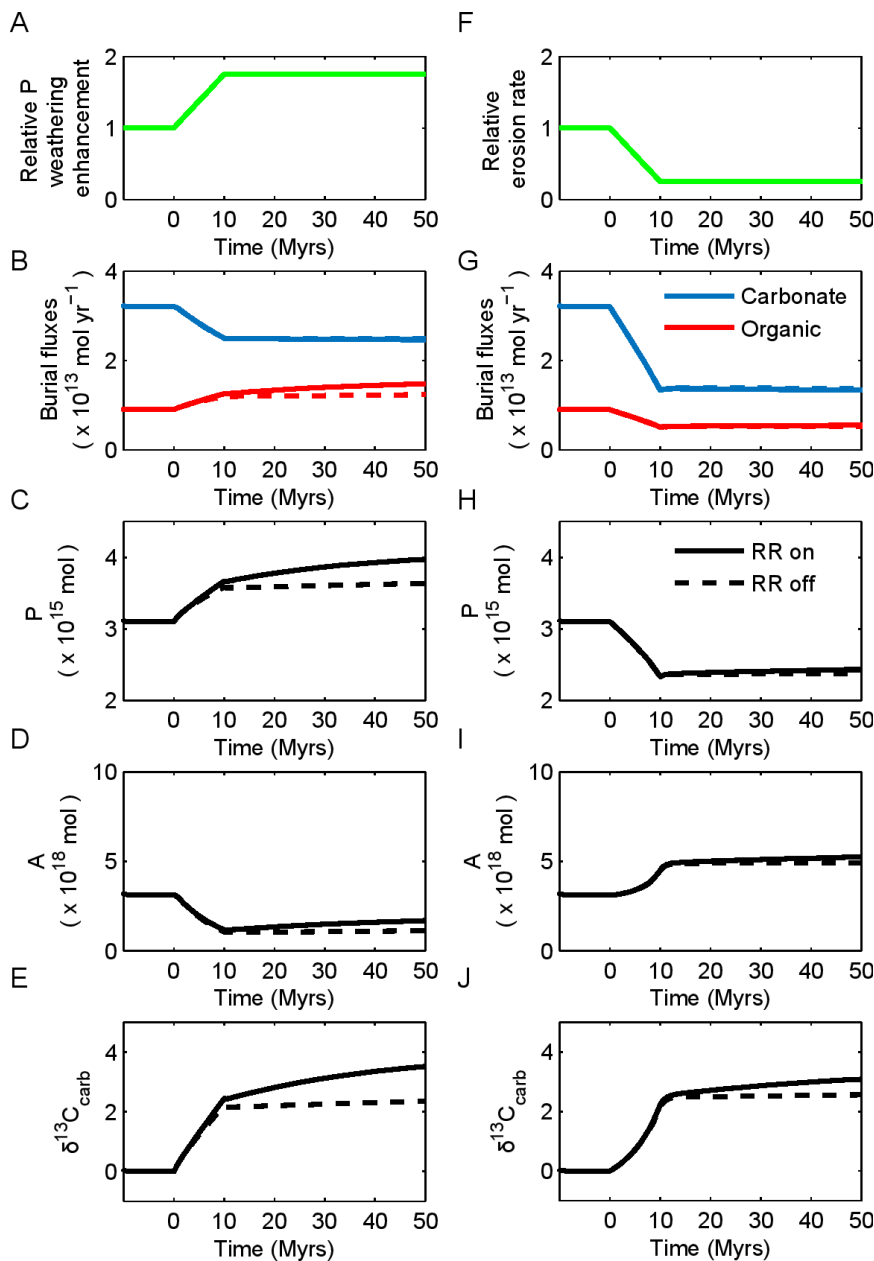
$$\delta^{13}\text{C}_{\text{carb}} = (F_{\text{bg}} \times \Delta B) / F_{\text{total}} + \delta^{13}\text{C}_{\text{in}} \quad (3)$$

Taking average values from the literature for carbon fluxes ($F_{\text{wg}} = 7.75 \times 10^{12} \text{ mol/yr}$, $F_{\text{wc}} = 24 \times 10^{12} \text{ mol/yr}$, $F_{\text{mg}} = 1.25 \times 10^{12} \text{ mol/yr}$, $F_{\text{mc}} = 8 \times 10^{12} \text{ mol/yr}$, $F_{\text{bg}} = 9 \times 10^{12} \text{ mol/yr}$, $F_{\text{total}} = F_{\text{wc}} + F_{\text{mc}} + F_{\text{wg}} + F_{\text{mg}} = 41 \times 10^{12} \text{ mol/yr}$ (19, 27), equation (3) suggests that trends in the long-term $\delta^{13}\text{C}$ average of $\sim -1\text{‰}$ to $\sim +5\text{‰}$ can be explained by varying the carbonate weathering flux between 1.5 times and 0.2 times the present day rate, respectively, without requiring any change in the rate of organic carbon burial. Such changes are within the limits of published estimates based on the Sr isotope record and/or sedimentation rates (see SI). Note that this mechanism does not require changes in $\delta^{13}\text{C}_{\text{in}}$.

Modelling the carbon isotope mass balance

To illustrate this idea, we compute the steady states of the long-term carbon cycle model with respect to the relative global erosion rate (Figure 3). The flux calculations follow the GEO-CARB and COPSE models (6, 26) under present day conditions, including both direct erosion and temperature effects on weathering fluxes. The isotope mass balance calculations in our model do not differ from those employed in Berner's analysis (5), but critically our model takes into account the effects of erosion on carbonate weathering. This is in line with the above discussion, and with direct evidence for considerable carbonate weathering in areas of high erosion and relief, e.g. the mountainous and foreland areas of the Andes (28). See SI for further model discussion.

An important consideration in this work is that changes in erosion rate also alter the rate of organic carbon burial via changes to the phosphorus cycle. To explore this further we link the rate of organic carbon burial in the model to the availability of phosphorus (22, 6). Phosphorus enters the surface system via the weathering of silicate, carbonate and organic C-bearing rocks, and the strength of the relationship between erosion and organic C burial depends on the P delivery from the weathering of each individual rock type.



PDF

Fig. 4. Comparison of positive $\delta^{13}\text{C}$ excursions driven by burial and erosion events. Panels show A: Relative model forcing factor. B, Burial fluxes for carbonate (F_{bc} , blue) and organic carbon (F_{bg} , red). C, Ocean phosphate. D, Atmosphere and ocean carbon. E, $\delta^{13}\text{C}$ of atmosphere/ocean carbon reservoir. Panels F-J repeat these quantities for the second model scenario. A positive $\delta^{13}\text{C}$ excursion is driven by increased organic carbon burial, via enhancement of phosphorus weathering (A-E), and is compared to a positive $\delta^{13}\text{C}$ excursion driven by a change in erosion (F-J). Both forcings (green lines) are ramped over a 10 Myr period, beginning at $t=0$. Solid lines show rapid recycling model (RR on, see text), dashed lines show no rapid recycling. Note that the positive excursion driven by organic C burial is associated with a decrease in atmosphere/ocean carbon (panel D), whilst the excursion driven by erosion is associated with an increase in the carbon reservoir (panel I). P input from weathering follows Hartmann et al. (2014) (29). Full model output is included in the SI.

Recent studies of P delivery from different rock types (29, 30) suggest that silicates play the major role, delivering more than 50% of riverine P (see SI). The model run showing this setup (M1) is shown in bold in figure 3. When the weathering of silicates is chiefly responsible for P delivery, an increase in erosion will not greatly affect the steady state P delivery or organic C burial, because the global silicate weathering rate is tightly controlled at steady state by the rate of CO_2 release (which remains constant in the model), and by any imbalance in the organic C cycle.

Dashed lines in figure 3 show results when silicates are assumed to contribute only $\sim 17\%$ of global P delivery (M2), as was assumed in the original COPSE model, based on crustal inventories rather than supply rates (6). The dotted lines (M3) show a more extreme case where all P delivery results from carbonate weathering. These configurations show that if most P is supplied by the weathering of carbonates, or follows a similar erosional forcing to carbonates (i.e. preferentially weathered at

high erosion rates) (25), then an increase in erosion rate would significantly increase P delivery, and therefore organic C burial, at steady state. This would act to counter the direct effect of increased erosion and carbonate weathering/deposition on $\delta^{13}\text{C}$, but only as far as carbon mass balance can allow.

We conclude from this analysis that changes in erosion rates most likely exert a powerful first-order control on long term carbonate $\delta^{13}\text{C}$, which is only partially nullified by associated changes in the phosphorus cycle and organic carbon burial.

We acknowledge that the long-term effects of erosion on global P delivery and organic carbon burial are still poorly constrained. Uncertainties exist in the various temperature and erosion effects on individual chemical weathering fluxes, the degree of preferential chemical weathering of accessory apatite minerals, and the possibility that changes in sedimentation rate may impact organic carbon burial differently to the burial of carbonates. In particular, it has been proposed that increased rates of sedimen-

545 tation will enhance the preservation of buried organic carbon and
546 phosphorus (5). Our model calculates the rate of organic carbon
547 burial based on a relationship between ocean phosphate, new
548 production and sedimentation rate (31), but we have also run an
549 alternative model setup to further explore this idea, wherein we
550 strengthen this relationship by giving the burial rates of organic
551 carbon and phosphorus an additional linear dependence on the
552 global erosion rate. The model results for ocean phosphate con-
553 centration are altered under these assumptions, but the steady-
554 state burial rates of carbon and phosphorus are not affected,
555 as they are ultimately constrained by the supply flux of P from
556 weathering (see SI for more details).

557 Our model run M1 shows what we consider to be the current
558 best guess for these mechanisms (see SI for more details and
559 other model runs), but a model is not unequivocal proof, and
560 it is clearly theoretically possible for erosion to increase organic
561 C burial more than it increases the burial rate of carbonates
562 (e.g. model run M3). However, if this were the case we would
563 expect $\delta^{13}\text{C}$ values to increase with increasing erosion rates, but
564 this is effectively falsified by the anti-correlation of $\delta^{13}\text{C}$ and all
565 available erosion proxies. We therefore conclude that although
566 erosion rates must certainly increase the rate of P delivery and
567 organic C burial, such increases must be less than the increases to
568 the burial rate of carbonates.

569 Figure 4 shows a series of time-dependent model runs where
570 a +3‰ positive excursion in $\delta^{13}\text{C}$ is caused by either increasing
571 organic carbon burial (via increased P delivery), or decreasing
572 the erosion rate. Increasing $\delta^{13}\text{C}$ via an organic C burial event
573 (Figure 4. A-E) results in a decrease in the atmosphere/ocean
574 carbon reservoir, i.e. a decrease in atmospheric pCO_2 , and global
575 cooling. Driving a similar positive excursion via a reduction in
576 erosion rates (Figure 4. F-J) causes a warming event due to the
577 weakening of silicate weathering. Importantly, we show that a
578 positive $\delta^{13}\text{C}$ excursion may be coincident with either an increase,
579 or decrease in the rate of organic carbon burial. This should be a
580 serious consideration for work aiming to tie the C isotope record
581 to global biogeochemical events.

582 An important factor influencing the time-dependent re-
583 sponse of the model is the assumption of 'rapid recycling' of
584 isotope signals due to the predominant weathering of recently-
585 deposited sediments. This idea has been explored in early carbon
586 and sulphur cycle models (7), and is included in the GEOCARB
587 models (5). We include this effect here by reducing the size of the
588 crustal pools of organic carbon and carbonates to around 10% of
589 the total crustal inventory, allowing for much quicker variation in
590 isotopic composition (RR on, solid lines in figure 4). This follows
591 Berner (5, 7). Dashed lines assume no rapid recycling, i.e. that
592 the isotopic signature of weathered material represents the whole
593 crustal inventory. As may be expected, the rapid recycling model
594 acquires steady state around an order of magnitude quicker than
595 the non-RR model. However, the choice of models does not affect
596 the qualitative dynamics we wish to demonstrate.

597 The isotopic composition of carbon inputs ($\delta^{13}\text{C}_{\text{in}}$) is not
598 fixed in our model, but responds to the changing composition
599 of the crustal reservoirs. Although changes to $\delta^{13}\text{C}_{\text{in}}$ (e.g. due
600 to preferential weathering of high- $\delta^{13}\text{C}$ lithologies) have been
601 shown to drive C isotope excursions (20, 23), the mechanism
602 explored in this paper does not depend on variations in $\delta^{13}\text{C}_{\text{in}}$. As
603 an example we run the model with this parameter fixed (Figure
604 S7), which shows the same qualitative results.

605 Interrogating carbon isotope excursions

606 A positive carbon isotope excursion caused by changes to
607 the inorganic carbon cycle has different climatic effects from

608 one caused by increasing the burial rate of organics: notably an
609 increase in CO_2 and surface temperature, rather than a decrease.
610 Such testable distinctions allow us to constrain the causes of spe-
611 cific carbon isotope events, and suggest that major, but short-lived
612 $\delta^{13}\text{C}$ events, which coincide with global cooling, such as the late
613 Ordovician Hirnantian event, could potentially relate to excess
614 organic burial. The longer Permo-Carboniferous glaciations also
615 occurred at a time of generally high $\delta^{13}\text{C}$, and are thus consistent
616 with an elevated organic burial flux, perhaps associated with the
617 evolution of a modern land biota (32). However, relatively low
618 erosion rates throughout this period imply that rates of organic
619 C burial need not have been as high as previously thought –
620 potentially resolving conflicts over the prediction of hyperambi-
621 ent O_2 levels (5). By contrast, glaciation during the Cenozoic
622 is associated with decreasing $\delta^{13}\text{C}$, and so appears to be more
623 consistent with the notion that the erosional forcing of carbonate
624 deposition outweighed that of organic burial.

625 Some times of elevated $\delta^{13}\text{C}$ do not coincide with glacia-
626 tion, and this is the case for the post-glacial Lomagundi Event
627 of exceptionally high $\delta^{13}\text{C}$ during the Palaeoproterozoic. Such
628 high $\delta^{13}\text{C}$ values may result from a hugely increased oxidative
629 weathering flux (21), following the Great Oxidation Event, which
630 could have been self-sustained by oxygenic siderite (iron carbon-
631 ate) weathering (22). Although not related to decreased erosion
632 rates, the Lomagundi Event can still be viewed as a time of
633 proportionately higher net carbon flux relative to gross carbon
634 throughput, in the same way as we argue for other times of high
635 baseline $\delta^{13}\text{C}$, such as during the Tonian Period of supercontinent
636 peneplanation. Note that in none of these cases does high $\delta^{13}\text{C}$
637 imply net oxygenation. Previously, these well-established $\delta^{13}\text{C}$
638 events were first-order determinants in our understanding of
639 Earth's oxygenation history.

640 Despite our emphasis here on erosional controls on $\delta^{13}\text{C}$,
641 we view the carbon isotope mass balance as a proportional pa-
642 rameter, whereby changes to the long-term norm correspond to
643 changes in the proportion that carbonate weathering makes up
644 of the global carbon cycle. In this regard, the anti-correlation
645 between $\delta^{13}\text{C}$ and $^{87}\text{Sr}/^{86}\text{Sr}$ over the past billion years could reflect
646 the dependence of both these parameters on the competing
647 tectonic influences of volcanism versus uplift, rather than erosion
648 *per se*.

649 Conclusions

650 The carbon isotope record is most commonly viewed in terms
651 of changing organic carbon burial rates, and less in terms of
652 the proportional organic component of the carbon cycle. By
653 viewing $\delta^{13}\text{C}$ as a combination of net and gross carbon fluxes
654 (and removing the common assumption that carbonate / silicate
655 / organic weathering systematics are invariantly proportional),
656 we show that higher proportional organic burial (higher f_{org})
657 can result from a decreased global weathering (carbonate) flux
658 to the ocean and may not be driven directly by changes in the
659 organic carbon burial flux. Moreover, it appears that tectonic
660 controls may plausibly be the underlying drivers of carbon isotope
661 trends that were previously attributed either to organic carbon
662 burial or to the changing isotopic composition of carbon sources.
663 This is evidenced by the anti-correlation between carbonate $\delta^{13}\text{C}$
664 and erosion proxies such as $^{87}\text{Sr}/^{86}\text{Sr}$ and reconstructed sediment
665 abundance. There seems to be no systematic relationship between
666 $\delta^{13}\text{C}$ and oxygenation through carbon burial, and we suggest
667 therefore that the oxygenation history of the Earth be reassessed
668 on a case-by-case basis in order to better take into account the
669 distinction between net and gross fluxes.

670 1. Kump LR., Garrels RM (1986) Modeling Atmospheric O_2 in the Global Sedimentary Redox

681
682
683
684
685
686
687
688
689
690
691
692
693
694
695
696
697
698
699
700
701
702
703
704
705
706
707
708
709
710
711
712
713
714
715
716
717
718
719
720
721
722
723
724
725
726
727
728
729
730
731
732
733
734
735
736
737
738
739
740
741
742
743
744
745
746
747
748

Cycle. *American Journal of Science* 286: 337-360.

2. Bottrell SH, Newton, RJ (2006) Reconstruction of changes in global sulfur cycling from marine sulfate isotopes. *Earth Science Reviews* 75: 59-83.
3. Smith RW, Bianchi TS, Allison M, Savage C, Galy V (2015) High rates of organic carbon burial in fjord sediments globally. *Nat Geosci* 8: 450-453.
4. Berner RA, Canfield DE (1989) A new model for atmospheric oxygen over Phanerozoic time. *Amer J Sci* 289: 333-361.
5. Berner RA (2006) GEOCARBSULF: A combined model for Phanerozoic atmospheric O₂ and CO₂. *Geochim et Cosmochim Acta* 70: 5653-5664.
6. Bergman NM, Lenton TM, Watson AJ (2004) COPSE: A new model of biogeochemical cycling over Phanerozoic time. *Amer J Sci* 304: 397-437.
7. Berner RA (1987) Models for carbon and sulfur cycles and atmospheric oxygen: application to Paleozoic geologic history. *Amer J Sci* 287: 177-196.
8. Karhu JA, Holland HD (1996) Carbon isotopes and the rise of atmospheric oxygen. *Geology* 24: 867-870.
9. Holland HD (2002) Volcanic gases, black smokers, and the Great Oxidation Event. *Geochim et Cosmochim Acta* 66: 3811-3826.
10. Knoll AH, Hayes JM, Kaufman AJ, Swett K, Lambert IB (1986) Secular variations in carbon isotope ratios from Upper Proterozoic successions of Svalbard and East Greenland. *Nature* 321: 832-838.
11. Des Marais DJ, Strauss H, Summons RE, Hayes JM (1992) Carbon isotope evidence for the stepwise oxidation of the Proterozoic environment. *Nature* 359: 605-609.
12. Berner RA (2009) Phanerozoic atmospheric oxygen: new results using the GEOCARBSULF model. *Amer J Sci* 309: 603-606.
13. Lyons TW, Reinhard CT, Planavsky NJ (2014) The rise of oxygen in Earth's ocean and atmosphere. *Nature* 506: 307-315.
14. Schrag DP, Higgins JA, Macdonald FA, Johnston DT (2013) Authigenic Carbonate and the History of the Global Carbon Cycle. *Science* 339: 540-543.
15. Hayes JM, Waldbauer JR (2006) The carbon cycle and associated redox processes through time. *Phil. Trans. R. Soc. B* 361: 931-950.
16. Campbell IH, Allen CM (2008) Formation of supercontinents linked to increases in atmospheric oxygen. *Nat Geosci* 1: 554-558.
17. Galy V, Peucker-Ehrenbrink B, Eglington T (2015) Global carbon export from the terrestrial biosphere controlled by erosion. *Nature* 521: 204-207.
18. Garrels RM, Lerman A (1984) Coupling the sedimentary sulfur and carbon cycles - an improved model. *Amer J Sci* 284: 989-1007.
19. Berner RA (1991) A model for atmospheric CO₂ over Phanerozoic time. *Amer J Sci* 291: 339-376.
20. Kump LR, Arthur MA (1999) Interpreting carbon-isotope excursions: carbonates and organic matter. *Chem Geol* 161: 181-198.
21. Bekker A, Holland HD (2012) Oxygen overshoot and recovery during the early Paleoproterozoic. *EPSL* 317-318: 295-304.
22. Bachan A, Kump LR (2015) The rise of oxygen and siderite oxidation during the Lomagundi Event. *Proc Natl Acad Sci USA* 112: 6562-6567.
23. Kump LR et al (1999) A weathering hypothesis for glaciation at high atmospheric pCO₂ during the late Ordovician. *Palaeogeog, Palaeoclimat, Palaeoecol* 152: 173-187.
24. Larsen IJ, Montgomery DR, Greenberg HM (2014) The contribution of mountains to global denudation. *Geology* 42: 527-530.
25. Jacobson AD, Blum JD (2003) Relationship between mechanical erosion and atmospheric CO₂ consumption in the New Zealand Southern Alps. *Geology* 31: 865-868.
26. Berner RA (1994) Geocarb II: A revised model of atmospheric CO₂ over Phanerozoic time. *Amer J Sci* 294: 56-91.
27. Kasting JF (2013) What caused the rise of atmospheric O₂? *Chem Geol* 362: 13-25.
28. Moquet J-S, et al (2011) Chemical weathering and atmospheric/soil CO₂ uptake in the Andean and Foreland Amazon basins. *Chem Geol* 287: 1-26.
29. Hartmann J, Moosdorf N, Lauerwald R, Hinderer M, West AJ (2014) Global chemical weathering and associated P-release - The role of lithology, temperature and soil properties *Chem Geol* 363: 145-163.
30. Compton J, et al (2000) Variations in the global phosphorus cycle. In *Marine Authigenesis: From Global to Microbial*, SEPM Special Publication 66: 21-33.
31. Van Cappellen P, Ingall ED (1994) Benthic phosphorus regeneration, net primary production, and ocean anoxia - a model of the coupled marine biogeochemical cycles of carbon and phosphorus *Paleoceanography* 9: 677-692.
32. Lenton TM et al (2016) Earliest land plants created modern levels of atmospheric oxygen. *Proc Natl Acad Sci USA* 113(35): 9704-9709.
33. Gradstein FM, Ogg JG, Schmitz MD, Ogg GM (Eds) *The Geologic Time Scale 2012: volume 1*. Elsevier, 435pp.

G.S.'s contribution was initiated at the WWU (Westfälische Wilhelms-Universität, Münster) during a stay as an Alexander von Humboldt research fellow from 2006-2008. His research was additionally supported by NERC grant NE/I00596X/1 and by a Chinese Academy of Sciences senior visiting researcher fellowship. B.M.'s contribution was supported by the Leverhulme Trust (RPG-2013-106) and a Leeds University Academic Fellowship. C-isotope

34. Hay WW et al (2006) Evaporites and the salinity of the ocean during the Phanerozoic: Implications for climate, ocean circulation and life. *Palaeogeog, Palaeoclimat, Palaeoecol* 240: 3-46.
35. Hayes JM, Strauss H, Kaufman AJ (1999) The abundance of ¹³C in marine organic matter and isotopic fractionation in the global biogeochemical cycle of carbon during the past 800 Ma. *Chem Geol* 161: 103-125.
36. Veizer J (1985) Carbonates and ancient oceans: isotopic and chemical record on time scales of 10⁷ - 10⁸ years. In: *The carbon cycle and atmospheric CO₂: Natural variations, Archean to Present*. Eds: E.T. Sundquist, W.S. Broecker. *AGU Geophysical Monograph* 32: 595-601.
37. Worsley TR, Moody JB, Nance RD (1985) Proterozoic to Recent tectonic tuning of biogeochemical cycles. In: *The carbon cycle and atmospheric CO₂: Natural variations, Archean to Present*. Eds: E.T. Sundquist, W.S. Broecker. *AGU Geophysical Monograph* 32: 561-572.
38. Rothman DH (2002) Atmospheric carbon dioxide levels for the last 500 million years. *Proc Natl Acad Sci USA* 99: 4167-4171.
39. Brasier MD, Lindsay JF (2001) Did supercontinent amalgamation trigger the "Cambrian Explosion"? In: *The ecology of the Cambrian radiation*. Eds: A.Y. Zhuravlev, R. Riding. Columbia University Press, New York, pp. 69-89.
40. Squire RJ, Campbell IH, Allen CM, Wilson CJL (2006) Did the Transgondwanan supermountain trigger the explosive radiation of animals on Earth? *EPSL* 250: 116-133.
41. Bradley DC (2011) Secular trends in the geologic record and the supercontinent cycle. *Earth Sci Rev* 108: 16-33.
42. Peters SE, Gaines RR (2012) Formation of the 'Great Unconformity' as a trigger for the Cambrian explosion. *Nature* 484: 363-366.
43. Spencer CJ et al (2014) Proterozoic onset of crustal reworking and collisional tectonics: Reappraisal of the zircon oxygen isotope record. *Geology* 42: 451-454.
44. Berner RA (2004), *The Phanerozoic Carbon Cycle: CO₂ and O₂*, Oxford Univ. Press, New York, USA.
45. Dilek Y, Furnes H (2011) *Ophiolite genesis and global tectonics: Geochemical and tectonic fingerprinting of ancient oceanic lithosphere*. *GSA Bulletin* 123: 387-411.
46. Condie K (2011) *Earth as an evolving planetary system*. Elsevier Academic Press. Cambridge MA, USA.
47. Scotese CR (2001) *Atlas of Earth History. PALEOMAP project*. Arlington, TX, USA.
48. Cawood PA, Hawkesworth CJ, Dhuime B (2013) The continental record and the generation of continental crust. *GSA Bulletin* 125: 14-32.
49. Krissansen-Totton J, Buick R, Catling DC (2015) A statistical analysis of the carbon isotope record from the Archean to the Phanerozoic and implications for the rise of oxygen. *Amer J Sci* 315: 275-316.
50. Sleep NH, Zahnle K (2001) Carbon dioxide cycling and implications for climate on ancient Earth. *J Geophys Res* 106: 1373-1399.
51. Royer DL, Donnadieu Y, Park J, Kowalczyk J, Godderis Y (2014) Error analysis of CO₂ and O₂ estimates from the long-term geochemical model GEOCARBSULF. *Amer J Sci* 314: 1259-1283.
52. Mills B, Watson AJ, Goldblatt C, Boyle R, Lenton TM (2011) Timing of Neoproterozoic glaciations linked to transport-limited global weathering. *Nat Geosci* 4: 861-864.
53. Li G, Elderfield H (2013) Evolution of carbon cycle over the past 100 million years. *Geochim Cosmochim Acta* 103: 11-25.
54. Lenton TM, Watson AJ (2000) Redfield Revisited: 1) Regulation of nitrate, phosphate and oxygen in the ocean. *Global Biogeochemical Cycles* 14: 225-248.
55. Hartmann J, Dürr HH, Moosdorf N, Meybeck M, Kempe S (2012) The geochemical composition of the terrestrial surface (without soils) and comparison with the upper continental crust. *Int J Earth Sci* 101(1): 365-376.
56. Caldeira K, Kasting JF (1992) The life span of the biosphere revisited. *Nature* 360: 721-723.
57. Shields GA (2007) A normalised seawater strontium isotope curve: possible implications for Neoproterozoic-Cambrian weathering rates and the further oxygenation of the Earth. *eEarth* 2: 35-42.

Acknowledgements

G.S.'s contribution was initiated at the WWU (Westfälische Wilhelms-Universität, Münster) during a stay as an Alexander von Humboldt research fellow from 2006-2008. His research was additionally supported by NERC grant NE/I00596X/1 and by a Chinese Academy of Sciences senior visiting researcher fellowship. B.M.'s contribution was supported by the Leverhulme Trust (RPG-2013-106) and a Leeds University Academic Fellowship. C-isotope data were kindly provided by Matthew Saltzman (see ref 33) and shown as a 20 point moving average of 1 Myr bins over the Phanerozoic (Fig. 1).

data were kindly provided by Matthew Saltzman (see ref 33) and shown as a 20 point moving average of 1 Myr bins over the Phanerozoic (Fig. 1).